Supplementary Notes

Genes involved in flagella synthesis from *Desulfobacterium autotrophicum* HRM2 and *Candidatus* Magnetomorum sp. HK-1 were used to find homologues in the draft genome of the strain CR-1 in addition to the eggNOG analysis. None of the *flg*, *fla* and *fli* genes found in the genomes of *D. autotrophicum* and *Ca*. Magnetomorum sp. HK-1 have homologues in the genome of the ectosymbiont. Thus, it seems reasonable to state that MEB do not have the ability to synthesize flagella as suggested by the absence of flagella when cells are observed under the transmission electron microscope. A similar approach was used to search the major players in chemotaxis signal transduction pathway, i.e. the transmembrane methyl-accepting chemotaxis protein (MCP) receptors and cytosolic proteins (Che). Among all genes involved in this pathway detected in the genomes of *D. autotrophicum* and *Ca*. Magnetomorum sp. HK-1 none have homologues in the genome of the ectosymbiont.

The genome of strain CR-1 reveals the presence of a magnetosome gene cluster (MGC) in a region of 25 kb with features typical of a genomic island as previously described for MGC in magnetotactic bacteria[1,2]. Indeed, in the 5' and 3' vicinity of the MGC, two transposases (EPICR _30004 and EPICR _30007) and one integrase (EPICR_30052) were found. The majority of the magnetosome genes had a maximum similarity to those of *Desulfamplus magnetovallimortis* and *Ca*. Magnetomorum sp. HK-1 (Supplementary Table S2), the two most closely related magnetite-producing magnetotactic bacteria with their genome sequenced (Fig. 3b). Synteny of the magnetosome genes with those of *Desulfamplus magnetovallimortis*[3] and *Ca*. Magnetomorum sp. HK-1[4] is also reasonably conserved (Fig. 3d).

Supplementary References

1. Ullrich, S., Kube, M., Schübbe, S., Reinhardt, R. & Schüler, D. A hypervariable 130-kilobase genomic region of Magnetospirillum gryphiswaldense comprises a magnetosome island which undergoes frequent rearrangements during stationary growth. *J. Bacteriol.* **187**, 7176–7184 (2005).
2. Nakazawa, H. *et al.* Whole genome sequence of Desulfovibrio magneticus strain RS-1 revealed common gene clusters in magnetotactic bacteria. *Genome Res.* **19**, 1801–1808 (2009).

3. Lefèvre, C. T. *et al.* Comparative genomic analysis of magnetotactic bacteria from the Deltaproteobacteria provides new insights into magnetite and greigite magnetosome genes required for magnetotaxis. *Environ. Microbiol.* **15**, 2712–2735 (2013).
4. Kolinko, S., Richter, M., Glöckner, F.-O., Brachmann, A. & Schüler, D. Single-cell genomics reveals potential for magnetite and greigite biomineralization in an uncultivated multicellular magnetotactic prokaryote. *Environ. Microbiol. Rep.* **6**, 524–531 (2014).
5. Loy, A. *et al.* Oligonucleotide Microarray for 16S rRNA Gene-Based Detection of All Recognized Lineages of Sulfate-Reducing Prokaryotes in the Environment. *Appl. Environ. Microbiol.* **68**, 5064–5081 (2002).
6. Lücker, S. *et al.* Improved 16S rRNA-targeted probe set for analysis of sulfate-reducing bacteria by fluorescence in situ hybridization. *J. Microbiol. Methods* **69**, 523–528 (2007).
7. Edgcomb, V. P. *et al.* Identity of epibiotic bacteria on symbiontid euglenozoans in O2-depleted marine sediments: evidence for symbiont and host co-evolution. *ISME J.* **5**, 231–243 (2011).
8. Snaidr, J., Amann, R., Huber, I., Ludwig, W. & Schleifer, K. H. Phylogenetic analysis and in situ identification of bacteria in activated sludge. *Appl. Environ. Microbiol.* **63**, 2884–2896 (1997).
9. Monteil, C. L. *et al.* Accumulation and Dissolution of Magnetite Crystals in a Magnetically Responsive Ciliate. *Appl. Environ. Microbiol.* **84**, (2018).
10. Amann, R. I. *et al.* Combination of 16S rRNA-targeted oligonucleotide probes with flow cytometry for analyzing mixed microbial populations. *Appl. Environ. Microbiol.* **56**, 1919–1925 (1990).

Supplementary Video 1. Light microscope video showing south-seeking magnetic protists sampled from Carry-le-Rouet, Mediterranean Sea, swimming toward and aggregating at the edge of a hanging drop. Reversing the bar magnet so that the south magnetic pole is closest to the edge of the drop, conducts the organisms to rotate and swim in the opposite direction, toward the opposite edge of the drop. While some magnetic protists are stuck at the edge of the drop, most of them reverse their swimming direction when the polarity of the bar magnet is changed.

Supplementary Figures

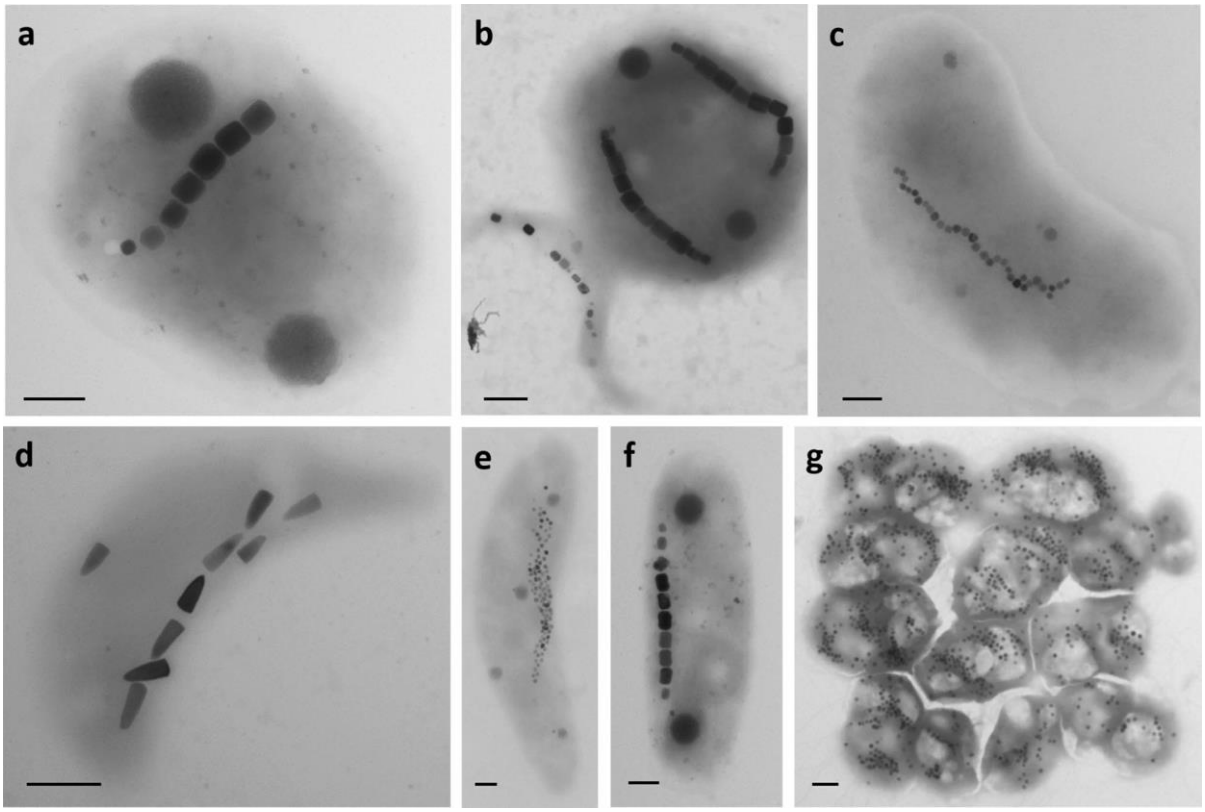

Supplementary Fig. 1. Transmission electron micrographs of north-seeking, free-living, magnetotactic cocci (**a**, **b**), spirillum (**b**), curved rods (**c**-**e**), rod (**f**) and multicellular prokaryotes (**g**), isolated from sediments collected from the Mediterranean Sea at Carry-le-Rouet, France. Scale bars represent 0.2 µm.

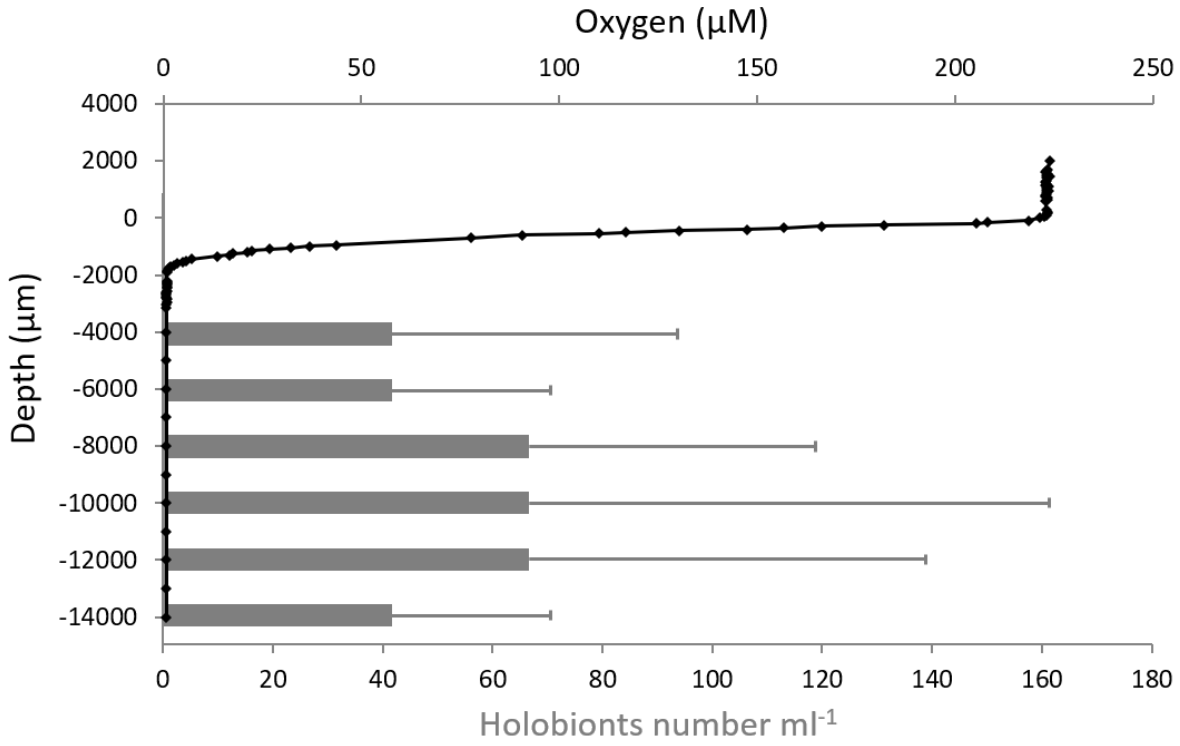

Supplementary Fig. 2. Vertical concentration profiles of oxygen and the magnetic protists through the water column and surface sediments of a bottle sample (microcosm) collected from Carry-le-Rouet, Mediterranean Sea. Note the measurements extend through the oxic–anoxic interface and the upper regions of the anaerobic zone of the sediment. Cell counts are reported as the mean of independent biological triplicate measurements and line extensions represent the positive standard deviation. The high variance is due to the technique used to count a low number of magnetic protist (see Methods).

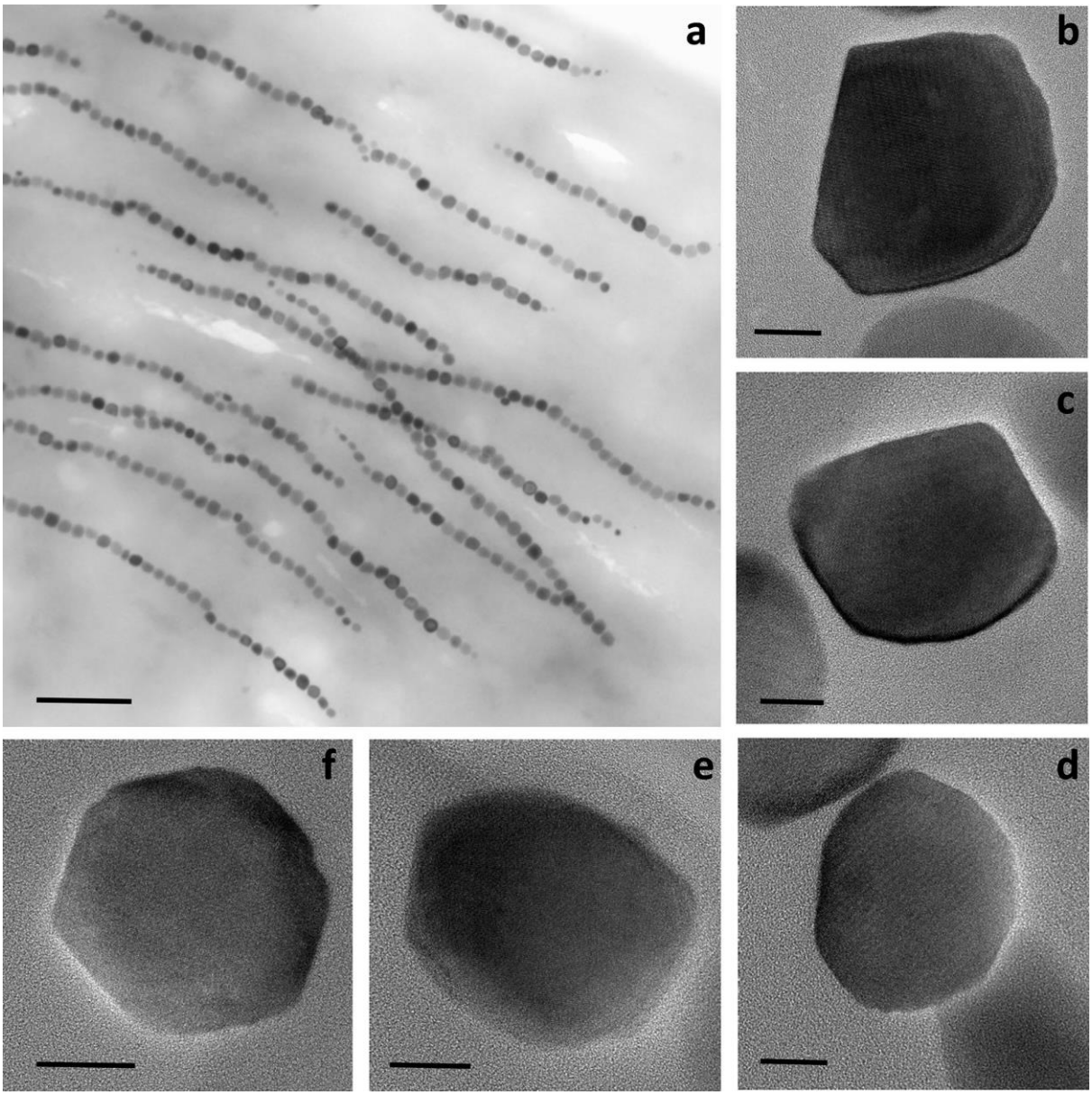

Supplementary Fig. 3. Transmission electron microscope (TEM) (**a**) and high-resolution TEM (**b-f**) images of magnetosomes produced by the ectosymbiotic magnetic bacteria collected from Carry-le-Rouet, showing the organization of the magnetosomes within the prokaryotic cells and their non-isometric, prismatic morphologies. Interestingly, magnetosomes from the same chain exhibit some variations of shape. Scale bars represent 500 nm (**a**) and 20 nm (**b-f**).

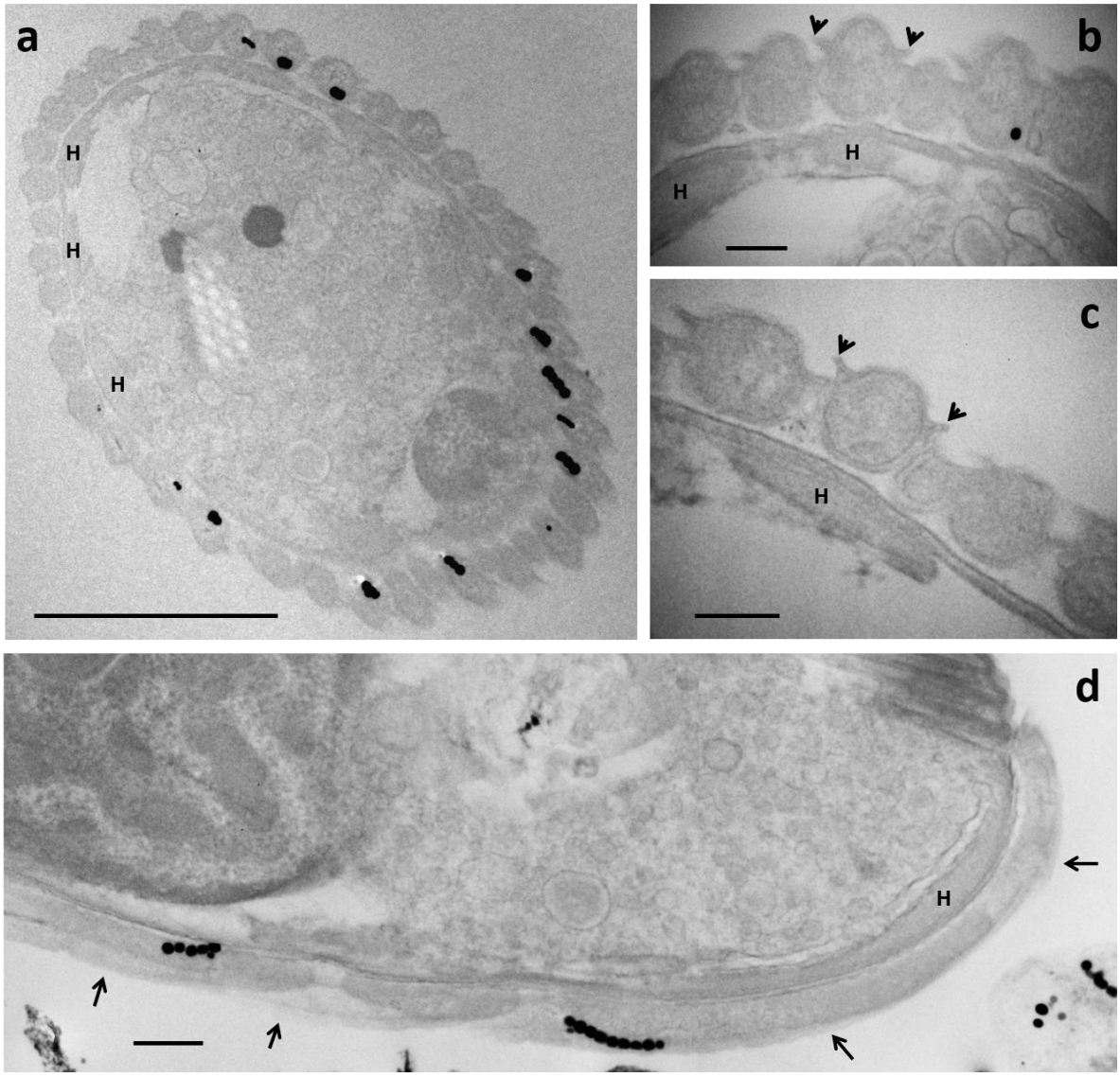

Supplementary Fig. 4. Transmission electron micrographs showing the organization and ultrastructure of the ectosymbiotic magnetic bacteria isolated from Carry-le-Rouet. **a**, Cross section of a magnetic consortium showing the presence of 41 bacteria surrounding the euglenozoan host. **b**, **c**, Cross sections of the ectosymbiotic bacteria showing their ultrastructure and their disposition at the surface of their host. Wing-like projections are shown with arrowheads. **d**, Longitudinal section of the ectosymbiotic bacteria showing possible mucilage (arrows) at the surface of the prokaryotic cell. In all panels, **H** represents hydrogenosomes. Scale bars represent 2 µm (**a**), 0.2 µm (**b** and **c**) and 0.5 µm (**d**).

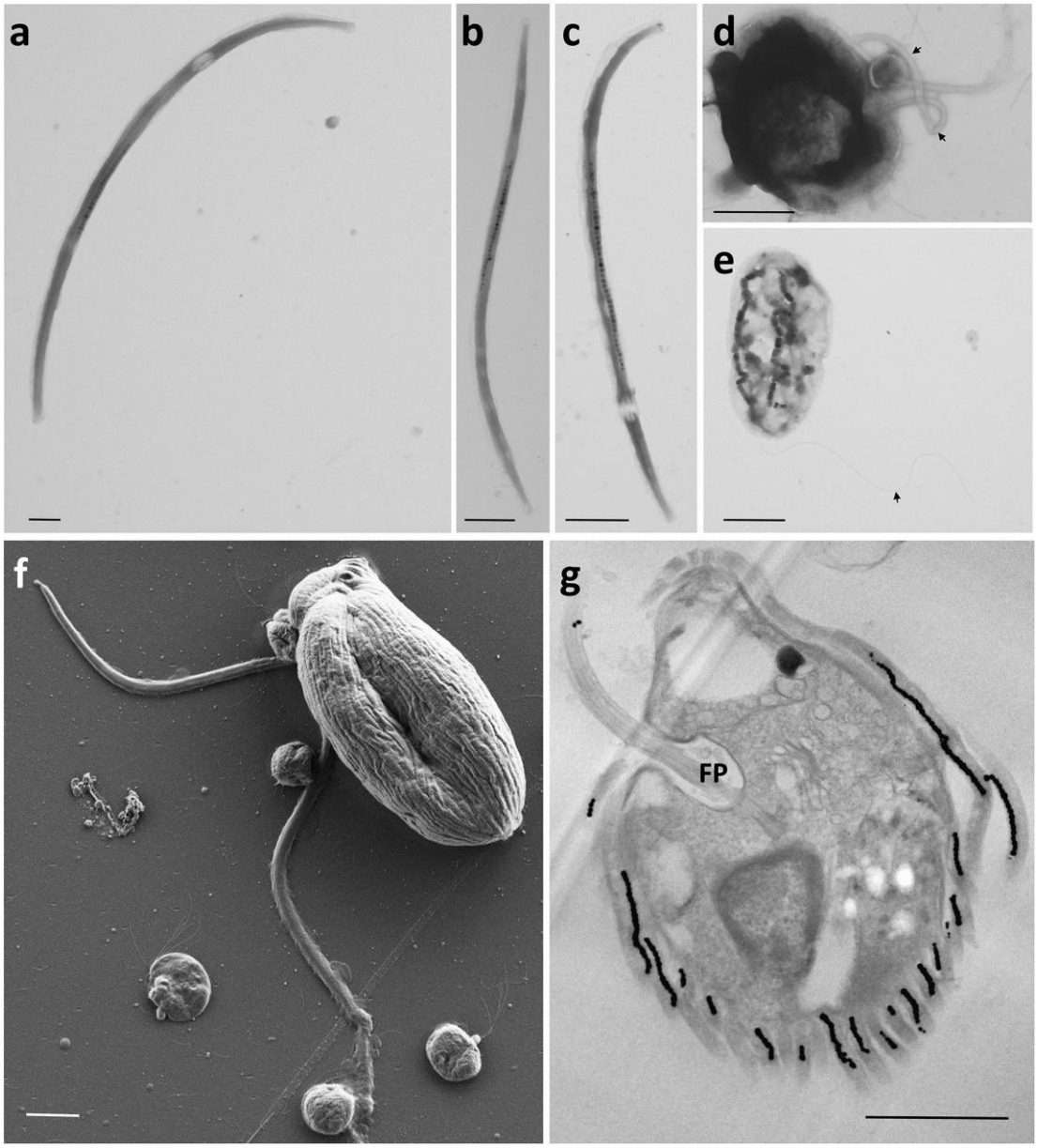

Supplementary Fig. 5. Transmission electron micrographs of magnetic ectosymbiotic bacteria detached from the surface of their host (**a**-**c**) and free-living magnetotactic bacteria (**d** and **e**) collected from the same sample in Carry-le-Rouet. Cells were negatively stained with uranyl acetate 1%, showing the absence of flagella surrounding the ectosymbionts while for the magnetotactic bacteria two flagella bundles (**e**) and one single polar flagellum (**f)** are observed (black arrows). **f**, Scanning electron image of a magnetic protist isolated from Carry-le-Rouet showing the presence of two thick flagella belonging to the protist. In comparison bundle of thin flagella can be seen around bacteria surrounding the magnetic protist. **g**, Transmission electron microscope of a thin-sectioned magnetic protist isolated from Carry-le Rouet showing that these flagella emerge from a flagellar pocket (**FP**). Scale bars represent 0.5 µm (**a**-**e**) and 2 µm (**f**, **g**).

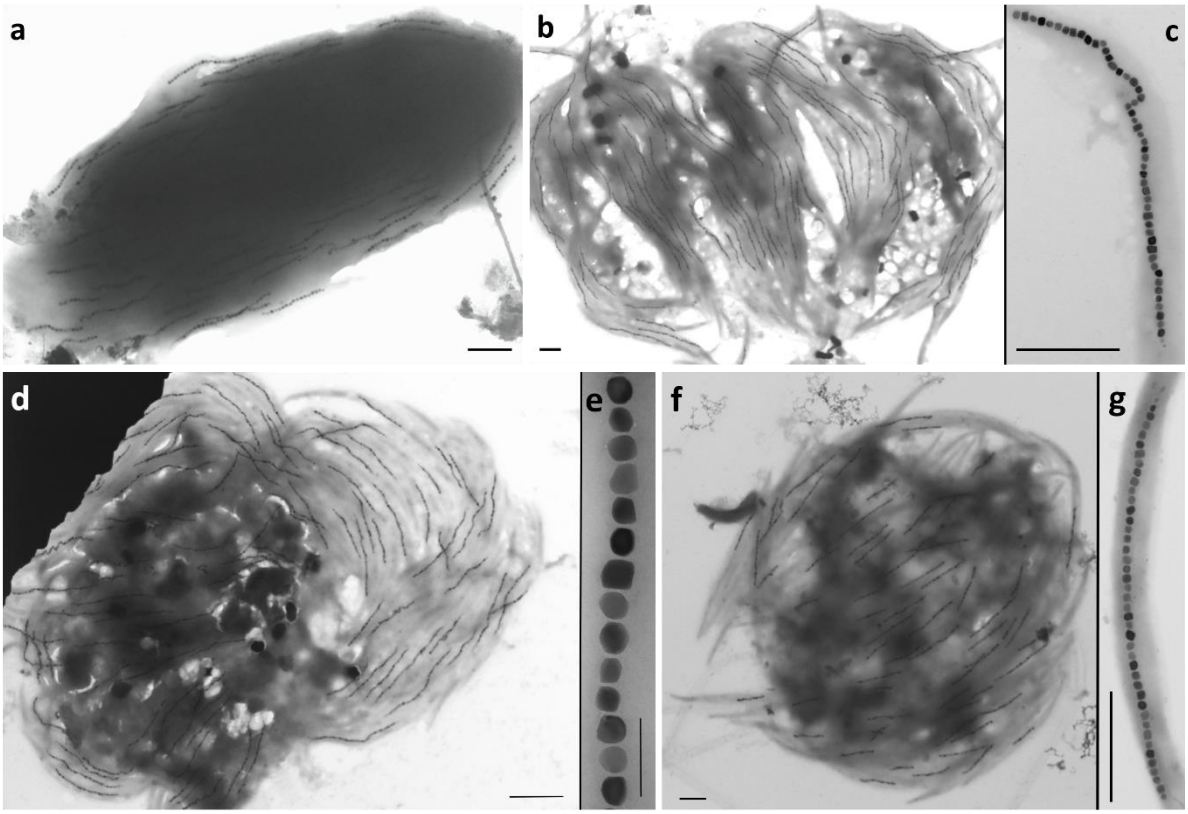

Supplementary Fig. 6. Transmission electron micrographs of south-seeking (**a**, **b**, **d**) or north-seeking (**f**) magnetic protists isolated from sediments collected in Port Leucate (**a**), Port de Boulouris (**b**), Cap de Creus (**d**) and Akaroa (**f**). Panels **c**, **e** and **g** are magnetosome chains of ectosymbionts from panels **a**, **b** and **d**, respectively. Scale bars represent 0.5 µm (**a**, **b**, **c**, **f** and **g**), 2 µm (**d**) and 200 nm (**e**).

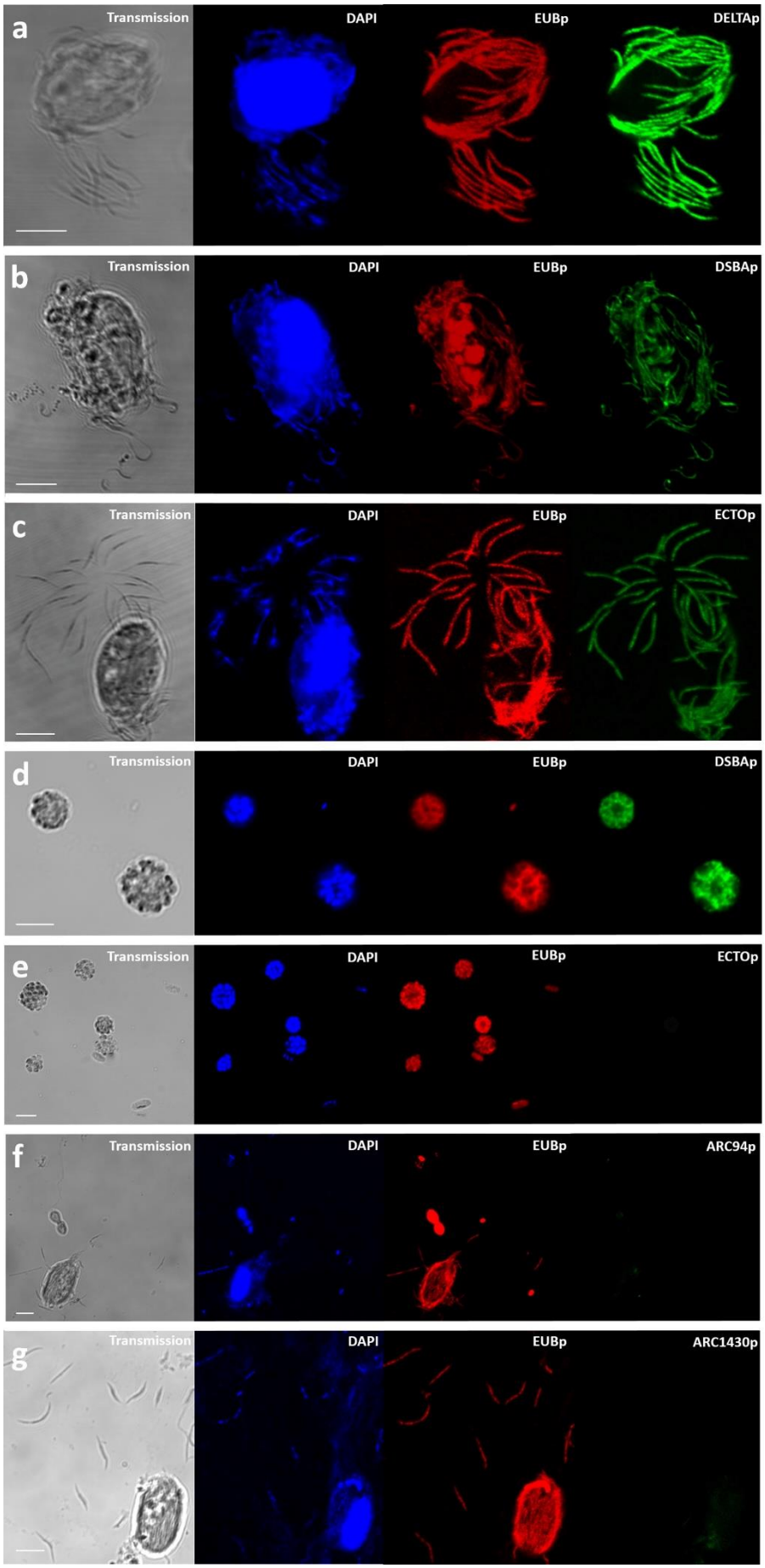
a
Transmission
DAPI
EUBp
DELTAp
b
Transmission
DAPI
EUBp
DSBAp
c
Transmission
DAPI
EUBp
ECTOp
d
Transmission
DAPI
EUBp
DSBAp
e
Transmission
DAPI
EUBp
ECTOp
f
Transmission
DAPI
EUBp
ARC94p
g
Transmission
DAPI
EUBp
ARC1430p

Supplementary Fig. 7. Fluorescence *in situ* hybridization (FISH) of magnetically collected protists from Carry-le-Rouet, Mediterranean Sea, showing that the ectosymbiotic bacteria is a deltaproteobacterium (**a**, probe DELTAp-ATTO488)[5] affiliated to the Desulfobacteraceae (**b**, DSBAp-ATTO488)[6] that hybridized with the ECTO-specific ATTO488-labeled probe ECTOp (5'- CAGTTTCTTCCCACTTGAC-3', complementary to nucleotides close to the 421 bp region of the 16S rRNA molecule of the ectosymbiotes) (**c**). The north-seeking multicellular magnetotactic bacteria present in the same sample as the magnetic protists were used as positive controls for DSBAp (**d)** and as negative controls for ECTOp (**e**). In order to discriminate from the ectosymbiotic bacteria previously identified from the surface of *C. aureus* and *B. bacati*[7], the *Arcobacter*-specific probes ARC94p (**f**) and ARC1430p (**g**)[8] were tested. Both probes did not hybridize the 16S rRNA gene sequence of the magnetic ectosymbiotic bacteria. Scale bars represent 5 µm.

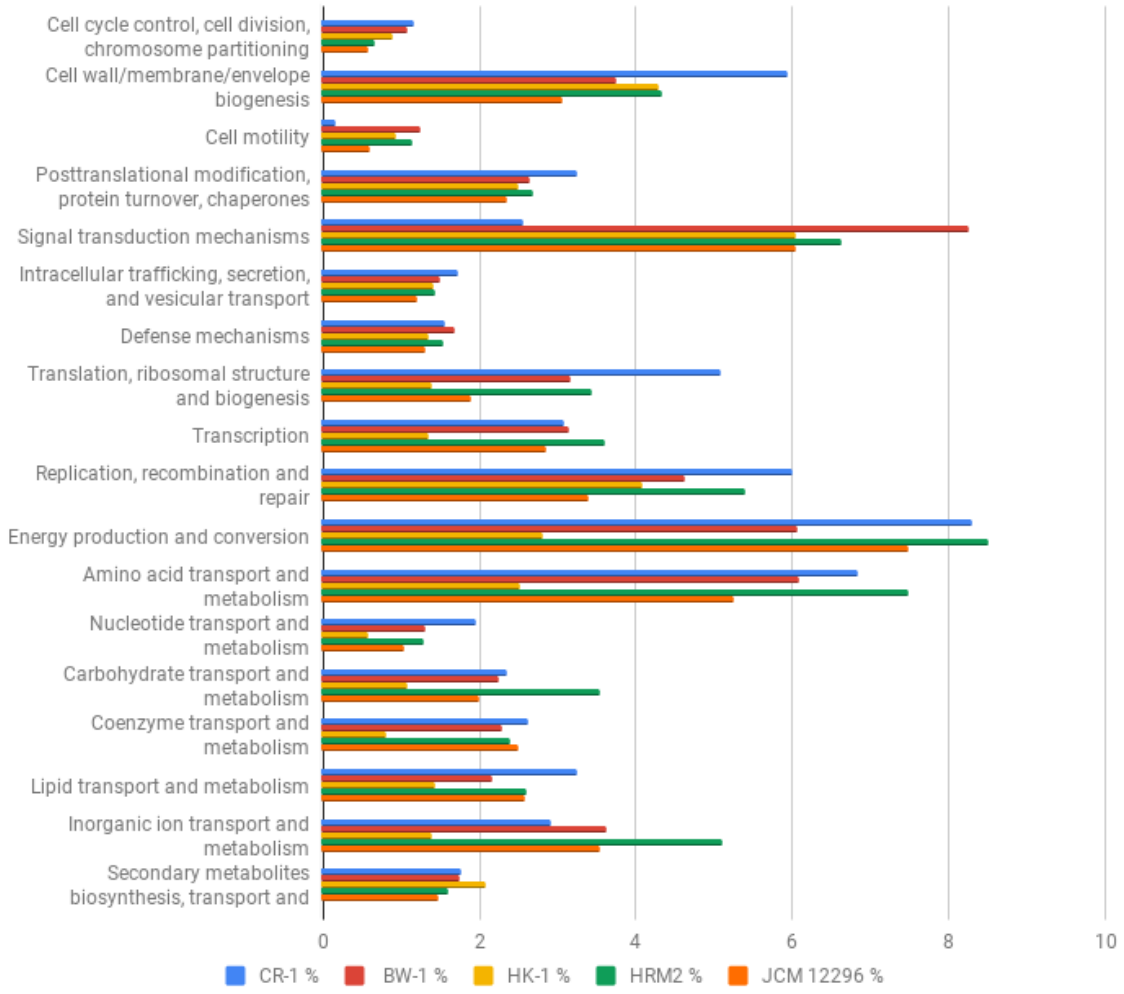

Supplementary Fig. 8. Functional classification of protein-coding genes from *Ca.* Desulfarcum epimagneticum compared to free-living magnetotactic and non- magnetotactic Desulfocateraceae species. This bar chart represents the percentage of protein-coding genes classified according to eggNOG functional categories for *Ca.* Desulfarcum epimagneticum CR-1, *Desulfamplus magnetovallimortis* BW-1, *Ca.* Magnetomorum HK-1, *Desulfobacterium autotrophicum* HRM2 and *Desulfosarcina cetonica* JCM 12296.

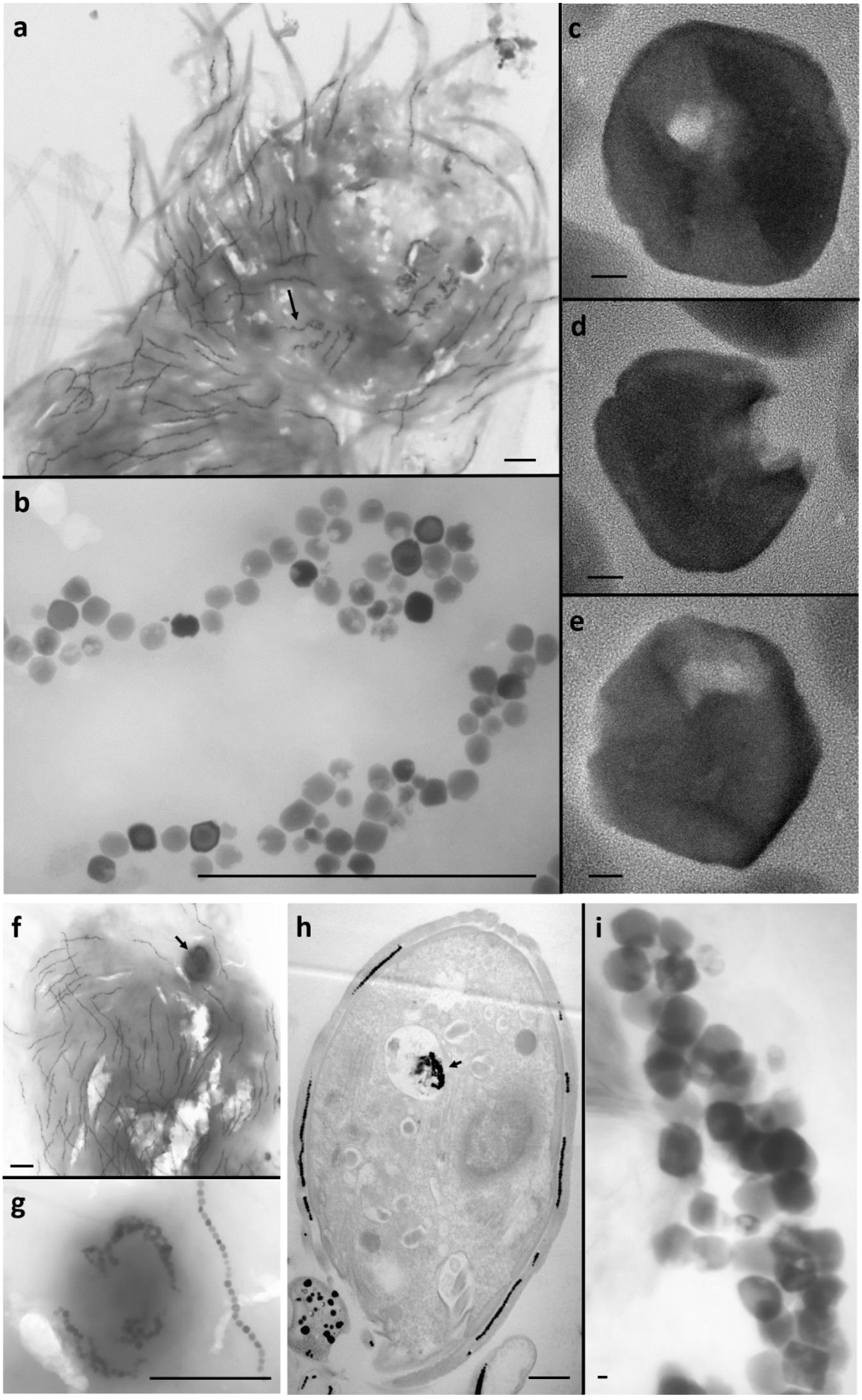
a
b
c
d
e
f
g
h
i

Supplementary Fig. 9. TEM images showing the presence of degraded magnetosomes inside euglenozoan hosts sampled from Carry-le-Rouet. Arrows in panels **a**, **f** and **h** indicate the position of the magnetosome chains shown in panels **b**, **g** and **i**, respectively. **c**-**e**, High-resolution TEM images of magnetite magnetosomes from panel **b**, showing structural defects due to partial dissolution, which has been previously reported for grazed magnetotactic bacteria[9]. Partially dissolved magnetosomes are similar to those biomineralized by the ectosymbionts, which indicates their ingestion by their host. Scale bars represent 1µm (**a**, **b**, **f**, **g** and **h**) and 10 nm (**c**-**e** and **i**).

Supplementary Tables

Supplementary Table 1. Comparison of size and number of CDS from 25 genomes of strains of the Desulfobacteraceae family indicates a genome reduction of *Ca*. Desulfarcum epimagneticum strain CR-1.

Strains	Genome size (Mb)	Number of CDS	% completion (CheckM)
Ca. Desulfarcum epimagneticum CR-1	3.26	3013	98.1
Ca. Magnetomorum sp. HK-1	14.59	12387	96.9
Ca. Magnetoglobus multicellularis str. Araruama	12.82	13649	98.2
Desulfatibacillum alkenivorans AK-01	6.52	5480	99.4
Desulfatibacillum alkenivorans DSM 16219	6.48	5330	98.1
Desulfatibacillum aliphaticivorans DSM 15576	6.48	5528	98.7
Desulfatitalea tepidiphila S28bF	5.62	5798	99.0
Desulfosarcina cetonica JCM 12296	7.15	10716	94.4
Desulfoluna spongiiphila AA1	6.54	6674	99.4
Desulfobacter postgatei 2ac9	3.97	3786	100
Desulfobacter vibrioformis DSM 8776	4.47	4030	96.1
Desulfobacter curvatus DSM 3379	5.67	5094	99.9
Desulfobacula toluolica Tol2	5.20	4912	99.4
Desulfobacula phenolica DSM 3384	4.88	4515	99.4
Desulfamplus magnetovallimortis BW-1	6.78	5610	96.9
Desulfobacterium autotrophicum HRM2	5.66	5200	99.4
Desulfobacterium vacuolatum DSM 3385	5.04	4288	98.7
Desulfotignum phosphitoxidans DSM 13687	5.00	4750	99.4
Desulfotignum balticum DSM 7044	5.12	4799	99.4
Desulfospira joergensenii DSM 10085	6.12	5542	99.4
Desulforegula conservatrix Mb1Pa	4.48	4303	99.4
Desulfofaba hansenii P1	6.73	5848	99.3
Desulfococcus oleovorans Hxd3	3.94	3592	99.4
Desulfococcus multivorans DSM 2059	4.42	4195	98.4
Desulfatirhabdium butyrativorans DSM 18734	4.49	3953	99.3
Desulfatiglans anilini DSM 4660	4.68	4745	99.4
Average	**6.06**	**5720**	**98.6**

Supplementary Table 3. 16S rRNA-targeted oligonucleotide probes used in this study.

Probe	Specificity	Sequence (5'-3') of probe	% FA	Reference
EUB338	Most Bacteria	GCTGCCTCCCGTAGGAGT	20 or 35	[10]
ECTO	Ectosymbiontes	CAGTTTCTTCCCACTTGAC	35	This study
DELTA495a	Most Deltaproteobacteria	AGTTAGCCGGTGCTTCCT	35	[5]
DSBA355	Most Desulfobacteraceae	CCATTGCGCAAAATTCCTCAC	35	[6]
ARC94	*Arcobacter*	TGCGCCACTTAGCTGACA	20	[8]
ARC1430	*Arcobacter*	TTAGCATCCCCGCTTCGA	20	[8]

Abbreviations: FA, formamide

Supplementary Table 2. List of proteins involved in metabolic pathways found in the draft genome of Ca. Desulfarcum epimagneticum strain CR-1.

Protein name/ gene number	Function	Size (amino acids)	Type bacterium with protein with highest sequence identity	Accession number	e-value	Coverage (%)	Identity (%)
AprA EPICR_10322	Sulphate-reduction	659	*Desulfatitalea tepidiphila*	WP_054029362	0	100	86
AprB EPICR_10323	Sulphate-reduction	145	*Desulfosarcina cetonica*	WP_054689150	2.00E-94	97	94
QmoA EPICR_10321	Sulphate-reduction	424	*Desulfatibacillum alkenivorans*	WP_012610700	0	99	82
QmoB EPICR_10320	Sulphate-reduction	778	*Desulfococcus multivorans*	WP_020877727	0	100	77
QmoC EPICR_10319	Sulphate-reduction	377	*Desulfatirhabdium butyrativorans*	WP_028323500	0	99	66
DsrA EPICR_30056	Sulphate-reduction	437	*Ca. Magnetoglobus multicellularis*	ETR70947	0	99	85
DsrB EPICR_30057	Sulphate-reduction	209	*Desulfobacterium vacuolatum*	WP_084067365	0	100	84
HynA EPICR_30147	Hydrogen oxidation	458	*Desulfatirhabdium butyrativorans*	WP_028324338	0	100	77
HynB EPICR_30145	Hydrogen oxidation	313	*Desulfatirhabdium butyrativorans*	WP_028324337	0	100	82
HynC EPICR_30148	Hydrogen oxidation	168	*Desulfosarcina cetonica*	WP_054699651	4.00E-73	95	68
CdhE EPICR_50265	CO_2 fixation	446	*Alkalispirochaeta odontotermitis*	WP_037563761	0	100	79
CdhC EPICR_50266	CO_2 fixation	737	*Alkalispirochaeta odontotermitis*	WP_037563760	0	100	84
CdhA EPICR_50267	CO_2 fixation	673	*Desulfobacula phenolica*	WP_092229394	0	98	84
CdhD EPICR_50268	CO_2 fixation	521	*Desulfococcus oleovorans*	WP_012176599	0	99	65
Unknown EPICR_30018	Magnetosome formation	132	*Ca.* Magnetomorum sp. HK-1	KPA16224	1.00E-13	65	34
MamK1 EPICR_30019	Magnetosome formation	362	*Magnetococcus marinus*	WP_011713881	3.00E-90	64	43

MamK2 EPICR_30020	Magnetosome formation	361	*Magnetospirillum magneticum*	WP_041039444	1.00E-103	67	45
Unknown EPICR_30021	Magnetosome formation	379	*Ca.* Magnetomorum sp. HK-1	KPA14592	2.00E-18	86	22
Mad10 EPICR_30022	Magnetosome formation	128	*Ca.* Magnetobacterium casensis	WP_040335342	5.00E-07	76	32
Unknown EPICR_30023	Unknown	55	-	-	-	-	-
Mad31 EPICR_30024	Magnetosome formation	310	*Ca.* Magnetobacterium bavaricum	KJU84849	2.00E-31	66	35
Mad30-1 EPICR_30025	Magnetosome formation	225	*Desulfonatronum lacustre*	WP_084031902	8.00E-102	96	64
MamI-1 EPICR_30026	Magnetosome formation	60	*Desulfamplus magnetovallimortis*	WP_080798181	1.00E-17	95	67
MamA EPICR_30027	Magnetosome formation	258	*Ca.* Magnetomorum sp. HK-1	KPA19039	7.00E-50	80	43
Mad1 EPICR_30028	Magnetosome formation	238	*Ca.* Magnetomorum sp. HK-1	KPA19040	6.00E-72	86	59
MamI-2 EPICR_30029	Magnetosome formation	120	*Desulfamplus magnetovallimortis*	WP_080798190	1.00E-28	94	48
MamQ EPICR_30030	Magnetosome formation	263	*Ca.* Magnetomorum sp. HK-1	KPA19042	4.00E-57	97	42
Mad2 EPICR_30031	Magnetosome formation	166	*Desulfamplus magnetovallimortis*	WP_080798196	5.00E-69	95	67
MamB EPICR_30033	Magnetosome formation	310	*Ca.* Magnetomorum sp. HK-1	KPA19045	3.00E-109	97	54
MamP EPICR_30034	Magnetosome formation	503	*Desulfamplus magnetovallimortis*	WP_080798201	9.00E-93	93	38
MamE-Cter EPICR_30035	Magnetosome formation	616	*Desulfamplus magnetovallimortis*	WP_080798204	3.00E-132	98	40
MamEO EPICR_30036	Magnetosome formation	611	*Ca.* Magnetomorum sp. HK-1	KPA19048	0	87	49
MamE-Nter EPICR_30037	Magnetosome formation	312	*Desulfonatronum thiodismutans st. ML-1*	AFZ77020	2.00E-74	98	46
Mad4 EPICR_30038	Magnetosome formation	148	*Ca.* Magnetomorum sp. HK-1	KPA19051	1.00E-17	85	39
Mad6 EPICR_30039	Magnetosome formation	286	*Desulfonatronum thiodismutans st. ML-1*	AFZ77023	9.00E-99	98	50
MamI-3 EPICR_30040	Magnetosome formation	132	*Ca.* Magnetomorum sp. HK-1	KPA16230	2.00E-11	65	37

MamL EPICR_30041	Magnetosome formation	90	*Ca.* Magnetomorum sp. HK-1	KPA16229	2.00E-18	97	46
MamM EPICR_30042	Magnetosome formation	302	*Desulfamplus magnetovallimortis*	WP_080798224	1.00E-113	94	58
Mad7 EPICR_30043	Magnetosome formation	152	*Desulfovibrio magneticus*	BAH77592	1.00E-06	82	33
Mad8 EPICR_30044	Magnetosome formation	119	*Desulfovibrio magneticus*	WP_015862720	6.00E-20	85	50
Mad23 EPICR_30045	Magnetosome formation	524	*Ca* . Magnetobacterium casensis	WP_040335329	1.00E-25	46	35
Mad9 EPICR_30046	Magnetosome formation	137	*Desulfonatronum thiodismutans st. ML-1*	AFZ77030	1.00E-40	95	51
Mad17-1 EPICR_30047	Magnetosome formation	647	*Desulfonatronum lacustre*	WP_028571663	0	99	61
Mad17-2 EPICR_200025	Magnetosome formation	679	*Ca.* Magnetobacterium bavaricum	KJU83258	0	93	46
Mad30-2 EPICR_200024	Magnetosome formation	254	*Ca.* Magnetobacterium casensis	KJU83257	2.00E-80	96	48

Ca.: Candidatus; st.: strain; sp.: specie